Biogeosciences, 19, 3523–3536, 2022
https://doi.org/10.5194/bg-19-3523-2022
© Author(s) 2022. This work is distributed under
the Creative Commons Attribution 4.0 License.

Biogeosciences Open Access EGU

Unprecedented summer hypoxia in southern Cape Cod Bay: an ecological response to regional climate change?

Malcolm E. Scully[1], W. Rockwell Geyer[1], David Borkman[2], Tracy L. Pugh[3], Amy Costa[4], and Owen C. Nichols[4]

[1]Applied Ocean Physics and Engineering, Woods Hole Oceanographic Institution, Woods Hole, MA, 02543, USA
[2]Rhode Island Department of Environmental Management, Providence, RI, 02908, USA
[3]Massachusetts Division of Marine Fisheries, New Bedford, MA, 02744, USA
[4]Department of Ecology, Center for Coastal Studies, Provincetown, MA, 02657, USA

Correspondence: Malcolm E. Scully (mscully@whoi.edu)

Received: 14 February 2022 – Discussion started: 21 February 2022
Revised: 3 June 2022 – Accepted: 9 June 2022 – Published: 28 July 2022

Abstract. In late summer 2019 and 2020 bottom waters in southern Cape Cod Bay (CCB) became depleted of dissolved oxygen (DO), with documented benthic mortality in both years. Hypoxic conditions formed in relatively shallow water where the strong seasonal thermocline intersected the sea floor, both limiting vertical mixing and concentrating biological oxygen demand (BOD) over a very thin bottom boundary layer. In both 2019 and 2020, anomalously high sub-surface phytoplankton blooms were observed, and the biomass from these blooms provided the fuel to deplete sub-pycnocline waters of DO. The increased chlorophyll fluorescence was accompanied by a corresponding decrease in sub-pycnocline nutrients, suggesting that prior to 2019 physical conditions were unfavorable for the utilization of these deep nutrients by the late-summer phytoplankton community. It is hypothesized that significant alteration of physical conditions in CCB during late summer, which is the result of regional climate change, has favored the recent increase in sub-surface phytoplankton production. These changes include rapidly warming waters and significant shifts in summer wind direction, both of which impact the intensity and vertical distribution of thermal stratification and vertical mixing within the water column. These changes in water column structure are not only more susceptible to hypoxia but also have significant implications for phytoplankton dynamics, potentially allowing for intense late-summer blooms of *Karenia mikimotoi*, a species new to the area. *K. mikimotoi* had not been detected in CCB or adjacent waters prior to 2017; however, increasing cell densities have been reported in subsequent years, consistent with a rapidly changing ecosystem.

1 Introduction

The occurrence of coastal hypoxia is increasing worldwide, and this rapid expansion is often linked to anthropogenic nutrient inputs (Diaz, 2001). Hypoxia caused by eutrophication is generally found in coastal regions that receive large freshwater inputs and the associated terrestrial nutrients (Fennel and Testa, 2019). Low dissolved oxygen (DO) also occurs in coastal waters not directly impacted by large freshwater inputs. For example, hypoxia on continental shelves can result from the upwelling of deep, nutrient-rich waters that enhance surface productivity and deliver oxygen-poor bottom waters to the shelf (Grantham et al., 2004). Long-term changes in hypoxia in these environments may be associated with long-term changes in the wind forcing and the associated changes in upwelling dynamics (Garcia-Reyes et al., 2015). Even in regions with high anthropogenic nutrient loading, variations in hypoxia are strongly influenced by variations in physical forcing so that both large-scale and regional climate variability can have important impacts on the occurrence of hypoxia in coastal waters (e.g., Scully, 2010). Processes such as wind forcing, water temperature, and vertical density stratification all play important roles in modulating bottom DO in a wide range of coastal environments (Wilson et al., 2008; Forrest et al., 2011; Yu et al., 2015; Scully, 2016). These physical processes control DO saturation (temperature) and horizontal advection and vertical mixing, which have direct impacts on the solubility and physical transport of DO and hence hypoxia.

Published by Copernicus Publications on behalf of the European Geosciences Union.

In addition to these direct impacts on physical transport, changes to the physical environment can significantly alter phytoplankton dynamics, which can also lead to hypoxia. Phytoplankton are the base of the marine food web, providing the organic carbon that ultimately drives hypoxia in most systems. Changes in vertical stratification, and its impacts on turbulent mixing, control light exposure and nutrient fluxes through the pycnocline impacting phytoplankton biomass, structure, seasonal dynamics, and taxonomic composition (Winder and Sommer, 2012). Increases in water temperature increase both light-saturated and light-limited rates of photosynthesis (Tilzer et al., 1986; Edwards et al., 2016) and can favor species that are better adapted to warmer waters. Increases in thermal stratification that result from warming surface waters generally decrease nutrient availability, which will favor species that are adapted to lower nutrient concentrations (Falkowski and Oliver, 2007) or can migrate to maintain their vertical position (Huisman et al., 2004). Thus, stronger vertical stratification is generally thought to favor dinoflagellates, including several species that form harmful algal blooms (HABs) (Smayda and Reynolds, 2001; Kudela et al., 2010). In addition to the toxic effects that can result in direct mortality, HABs also have been linked to hypoxia in a number of marine environments (O'Boyle et al., 2016; Griffith and Gobler, 2020).

Most HAB-forming species are dinoflagellates, and there is growing evidence that blooms of dinoflagellates are increasing in frequency, magnitude, and geographic extent, particularly in coastal environments (Anderson et al., 2012). Smayda (2002) proposes that the establishment of new bloom species results from a three-step process that includes regional translocation, colonization, and the achievement of competitive dominance. He concludes that translocation is not a sufficient condition for a non-indigenous species to bloom and that significant habitat disturbance is necessary for a new species to achieve competitive dominance (i.e., bloom). This link between habitat disturbance and bloom expansion is one reason why climate change has been hypothesized to play a key role in the overall increase in dinoflagellate blooms in coastal waters (Wells et al., 2020). In this paper we present observations of unprecedented bottom hypoxia in southern Cape Cod Bay (CCB) that is hypothesized to result from the emergence of a new late-summer bloom species – *Karenia mikimotoi*. Prior to 2017, *K. mikimotoi* had not been found in routine sampling but has become prevalent during the late-summer months. This dinoflagellate appears to be well-adapted to the environmental conditions found in southern CCB, which have changed significantly over the last several decades. We will present detailed observations of water column structure and the distribution of DO and chlorophyll fluorescence collected during the late summer of 2020 in order to highlight the physical conditions that favor bottom hypoxia. Long-term changes in chlorophyll fluorescence and species composition detected by ongoing environmental monitoring in CCB will be used to put the 2020 observations into context. Finally, we will demonstrate that CCB is experiencing dramatic changes in physical conditions during the summer months and will speculate on the role that regional climate change has played in this apparent regime shift.

2 Background

CCB is located at the southernmost extremity of the Gulf of Maine (GOM) and is influenced both by the offshore waters and by coastal waters moving through the inshore regions of Massachusetts Bay (Signell et al., 2000). CCB experiences significant seasonal variations in vertical density stratification, with well-mixed conditions observed for much of the late fall and winter and strong thermal stratification during summer (Geyer et al., 1992). The southwesterly winds that frequently occur during the summer result in upwelling along the western coast of the bay. Phytoplankton dynamics exhibit significant interannual variability, but there is often a late winter/early spring bloom in response to the increase in vertical density stratification in April (Oviatt et al., 2007). Surface chlorophyll is typically low during the summer, when surface waters are generally depleted of inorganic nutrients (Jiang et al., 2007). Strong mixing and destratification in the fall often result in a secondary bloom, driven primarily by the increased vertical flux of nutrients into the surface waters (Oviatt et al., 2007).

Long-term measurements of water properties conducted with the support of the Massachusetts Water Resources Authority (MWRA) provide a record of seasonal variability in vertical density stratification and DO in Massachusetts Bay and CCB extending back nearly 30 years (Libby et al., 2020). These data indicate that while there is always a decline in near-bottom DO in the late summer and early fall, the bays have never previously experienced hypoxia prior to the 2019 event. The lowest DO recorded in CCB before 2019 was $3.7\,\mathrm{mg\,L^{-1}}$, and the seasonal minimum is more typically between 5 and $6\,\mathrm{mg\,L^{-1}}$ (Xue et al., 2012). These long-term data also document a trend of warming surface waters that is consistent with the regional trend in the GOM (Pershing et al., 2015), the implications of which are discussed below.

CCB is home to a diverse assemblage of phytoplankton species. There are ~ 300 phytoplankton taxa that have been identified in the region, with a subset of ~ 30 species commonly reported (Hunt et al., 2010). Small ($< 10\,\mu\mathrm{m}$) unidentified microflagellates are numerically dominant throughout the year. Of the larger identifiable species, diatoms dominate through much of the winter, spring, and autumn but give way to dinoflagellates during the summer months when strong vertical density stratification is present. During the summer, dinoflagellates consist primarily of small species such as *Gymnodinium*, but larger species such as *Ceratium* also are commonly found. In recent years, the previously undetected dinoflagellate species *K. mikimotoi* has been detected with increasing cell densities in samples collected throughout the

GOM. *K. mikimotoi* is a planktonic dinoflagellate species responsible for harmful blooms in coastal waters worldwide. It grows well in low-light conditions and is particularly well suited to exploit light-limited environments (Li et al., 2019). It can vertically migrate up to $2.2\,\mathrm{m\,h^{-1}}$ (Koizumi et al., 1996), forming concentrated layers within the pycnocline that are $< 1\,\mathrm{m}$ in vertical thickness during a bloom (Dahl and Brockmann, 1989; Bjornsen and Nielsen, 1991; Brand et al., 2012). It has low nutritional value, and many phytoplankton feeders avoid ingesting this species (Schultz and Kiorboe, 2009). *K. mikimotoi* has strong allelopathy, which is enhanced when high cell concentrations are present (Riegman et al., 1996; Uchida et al., 1999). These allelopathic effects are thought to be an important mechanism that allows *K. mikimotoi* to become the dominant bloom species despite its relatively slow growth rate.

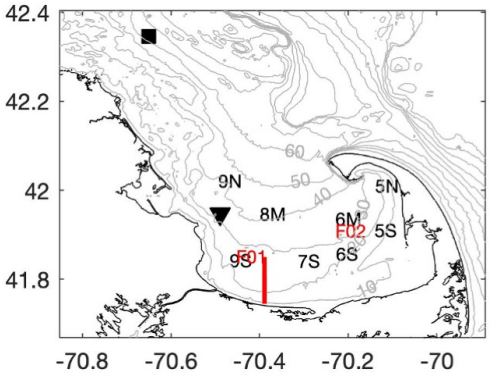

Figure 1. Map of Cape Cod Bay (CCB) showing the locations of the CCS monthly water quality stations (black letters), the MWRA sampling locations in CCB (red letters), NDBC buoy 44013 (black square), MDMF Wreck of the Mars bottom temperature sensor (black triangle), and the 2020 transect shown in Fig. 3 (red line). Grey contours are depths in meters.

3 Methods

In late summer 2019, in response to reports of significant lobster mortality in southern CCB by the local lobster fleet, Massachusetts Division of Marine Fisheries (MDMF) staff conducted an initial survey of bottom DO. On this survey, which was conducted on 25 and 26 September 2019, bottom DO was measured with a YSI 6920 V2-2 data sonde. Two subsequent surveys were conducted on 30 September and 1 October 2019 by the staff of the Center for Coastal Studies (CCS) and MDMF to provide greater spatial coverage. CCS staff used a YSI ProDSS multiparameter meter and CastAway-CTD. In response to the hypoxic conditions reported in 2019, increased ship-based sampling was conducted during late summer and early fall in 2020. The 2020 spatial surveys collected vertical profiles with an RBR CTD (conductivity, temperature, and depth) device equipped with a Rinko fast-response optical DO sensor, Turner Designs chlorophyll fluorometer, and Seapoint optical backscatter sensor (OBS). The CTD samples at 16 Hz and was lowered slowly by hand to the bottom, providing highly resolved vertical profiles of the entire water column. Surveys in 2020 were conducted on 31 August, 3, 10, 16, and 24 September, and 2 October. At select CTD profile locations, surface and bottle samples were collected and analyzed for extracted chlorophyll and dissolved inorganic nutrients. Extracted chlorophyll data were used to calibrate the vertical profiles of fluorescence, and the optical DO sensor was calibrated in the laboratory using a two-point linear regression obtained using fresh water with 100 % (obtained using aerating bubbler) and 0 % saturation (obtained by removing all DO by adding sodium sulfite).

In addition to these detailed data collected in 2019 and 2020, CCS staff have been collecting monthly water quality data at eight locations in CCB since 2006 (Fig. 1). While a variety of parameters were measured beginning in 2006, collection of full water column profiles of chlorophyll fluorescence and photosynthetically active radiation (PAR) began in 2011, when surveys included a Seabird SBE-19plus CTD equipped with an SBE-43 dissolved oxygen sensor, WET Labs ECO-FL fluorometer, and Biospherical QSP PAR sensor. The CTD samples at 4 Hz and is hand-lowered at a speed of $\sim 0.5\,\mathrm{m\,s^{-1}}$, stopping approximately 2–3 m above the bottom. In addition to the CTD data, CCS collects discrete bottle samples for inorganic nutrient analysis. Bottles at both the surface and 2–3 m above the bottom are collected. These samples are passed through a 0.4 µm membrane filter and frozen for subsequent laboratory analysis on an Astoria 2 autoanalyzer following the methods outlined in Costa et al. (2020).

The MWRA has been collecting water samples for phytoplankton identification and quantification at 34–48 locations throughout Boston Harbor, Massachusetts Bay, and CCB roughly every month since 1992. Each month, surface water samples are collected from two locations in CCB (F01 and F02). These samples are collected with a Niskin bottle, and a 1 L subsample is preserved with Lugol's solution. Phytoplankton samples are concentrated via gravitational setting by a factor of approximately 16 : 1 as described by Borkman et al. (1993), Borkman (1994), and Turner et al. (1995). A 1 mL aliquot of concentrate is transferred to a gridded Sedgwick–Rafter chamber, and phytoplankton are counted using an Olympus BH-2 research microscope with phase contrast optics following methods outlined in Costa et al. (2020). Species abundance estimates are derived from these counts following the methods outlined in Hunt et al. (2010).

To place these data into the context of regional climate change in CCB, we analyze several other sources of long-term data from the region. The National Data Buoy Center (NDBC) Boston (44013) buoy has measured surface water temperature and wind (speed and direction) hourly since Au-

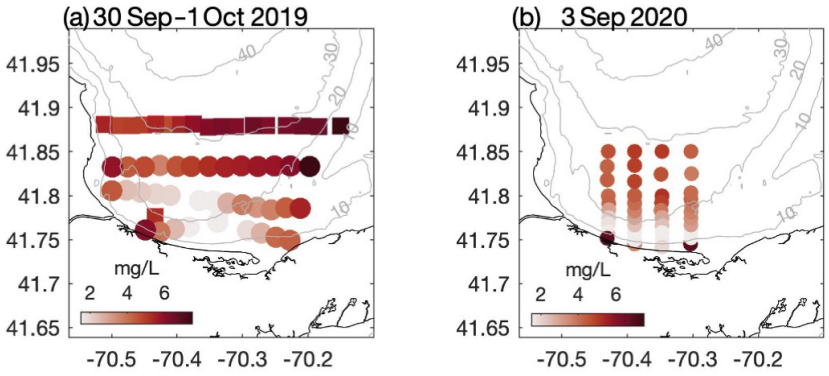

Figure 2. Bottom dissolved oxygen measured in southern CCB during late summer **(a)** 2019 and **(b)** 2020. In 2019 data were collected on 30 September (squares) and 1 October (circles). In both years a broad region of hypoxic bottom water developed in relatively shallow water where the thermocline intersects the seafloor. Grey contours are depths in meters.

gust 1984, providing over 36 years of nearly continuous data. The surface water temperature and wind measurements are made 1.1 m below and 3.2 m above the mean water surface, respectively. Similarly, the MDMF has maintained several bottom temperature loggers in CCB beginning in July 1991. These temperature loggers sample every 2 h, and here we analyze over 3 decades of bottom temperature measured at the Wreck of the Mars location in the northwest corner of CCB, where the local water depth is ~ 33 m (Fig. 1). While this bottom sensor and the NDBC station are not co-located, they provide information about the long-term trends in both surface and bottom temperature in the region. In the analysis presented below, we take averages over the summer months (June–September) and only include years when over 90 % of the data are available.

4 Results

The late-summer 2019 surveys conducted by MDMF and CCS staff revealed a broad area of hypoxic water in southern CCB (Fig. 2a). The region of hypoxia extended ~ 20 km in the along-isobath direction and at least 6 km in the across-isobath direction, spanning water depths from approximately 9 to 24 m. In interviews conducted by MDMF staff, mortality in lobster traps was reported beginning on 20 September 2019, and local scallop fishers reported significant mortality in scallop trawls conducted as early as 15 September 2019. A broad survey conducted on 8 October 2019 (not shown), following a period of relatively energetic winds from the north, found no hypoxic water in the region, suggesting that low-DO bottom waters either vertically mixed or were advected offshore. Increased sampling was conducted in 2020, which demonstrated that a broad region of bottom hypoxia formed for a second consecutive summer (Fig. 2b). Hypoxic conditions were first detected during an across-shelf survey conducted on 31 August 2020, which found bottom DO levels below 2 mg L^{-1} centered on the 20 m isobath (Fig. 3b). A more comprehensive spatial survey conducted on 3 September 2020 revealed that the hypoxic water extended at least 10 km in the along-isobath direction, with a general distribution largely consistent with late summer 2019. Hypoxic bottom waters persisted through 16 September 2020, but a survey conducted on 24 September 2020, after a period of sustained strong winds from the north, found bottom DO levels had increased to well above hypoxic levels.

The high-resolution sampling conducted during 2020 provided a detailed description of the distribution of DO, chlorophyll fluorescence, optical backscatter, and water column density structure (Fig. 3). On 31 August 2020, strong temperature stratification was present with a horizontal density front that intersected the bathymetry (Fig. 3b–d). The isotherms were approximately horizontal, capping a thin bottom boundary layer (BBL), that increased in height with increasing depth offshore. Low-oxygen water was confined to the thin BBL, with the lowest oxygen levels roughly coincident with the thinnest BBL heights associated with the bottom density front. A sub-surface chlorophyll maximum ($> 100\,\mu g\,L^{-1}$) was present in the pycnocline at a depth of roughly 20 m. The 31 August survey followed a period of moderate winds from the north (Fig. 3a). A second survey on 3 September, following a period of moderate winds from the south, demonstrated that the low-DO water was still present but had been advected shoreward with the lowest bottom DO centered on the 15 m isobath (Fig. 3e). The upwelling associated with southerly winds pulled colder bottom waters onshore and increased the thickness of the BBL. Weak southerly winds continued for most of the next week, providing sustained upwelling conditions, and the center of hypoxic water had advected even closer to shore on 10 September (Fig. 3h). Bottom DO levels in water depths between 20 and 30 m increased, and the total volume of hypoxic water decreased relative to the prior survey (Table 1). The survey conducted on 16 September 2020 followed a period

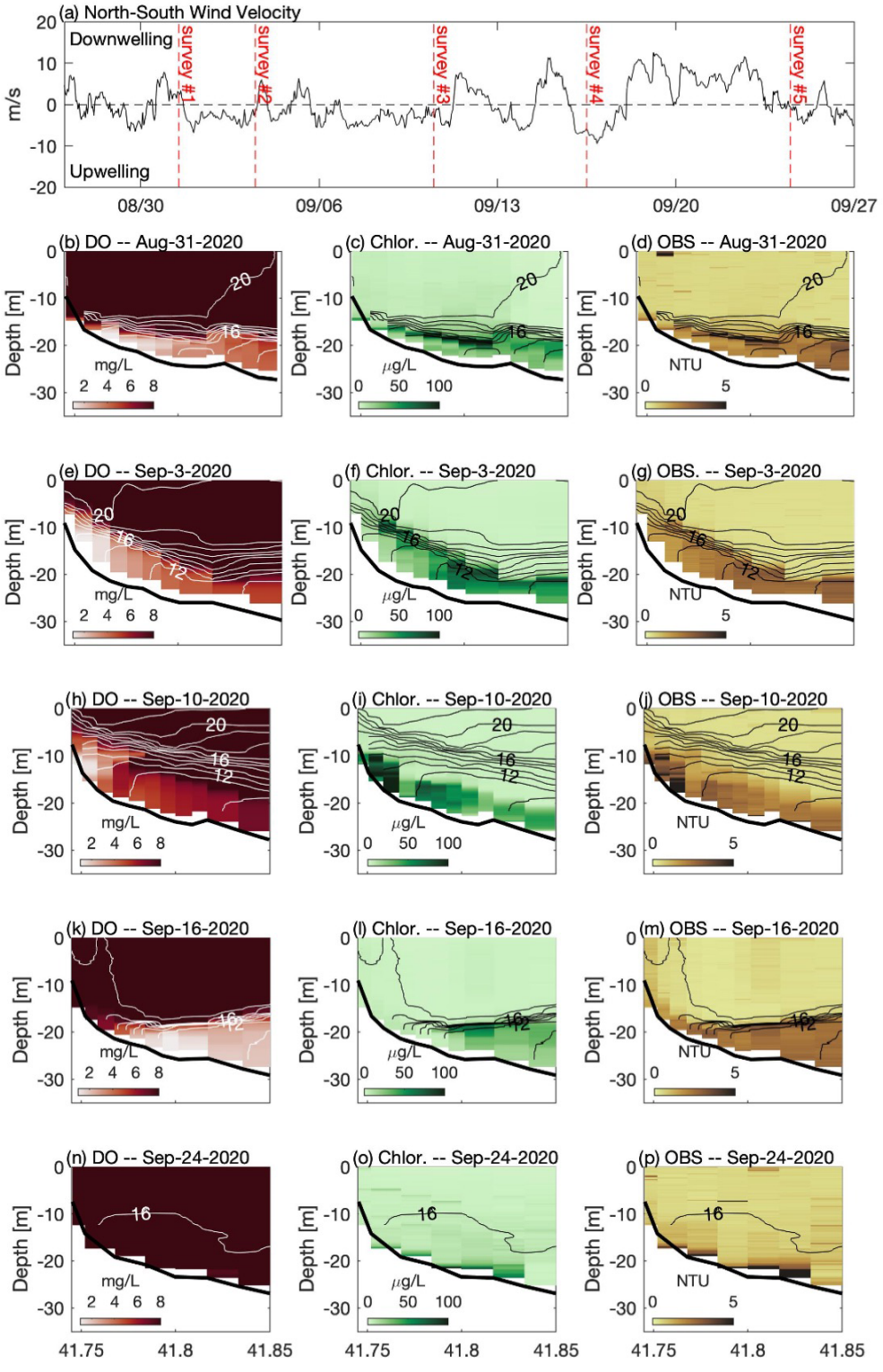

Figure 3. **(a)** North–south component of wind measured at NDBC buoy 44013. Panels on the left **(b, e, h, k, n)** show across-shelf transects of dissolved oxygen, panels in the center **(c, f, i, l, o)** show chlorophyll fluorescence, and panels on the right **(d, g, j, m, p)** show optical backscatter measured during a series of cruises in late summer 2020. For each transect, temperature contours (1 °C interval) are shown. In the top panel the vertical dashed red lines indicate the approximate timing of each cruise. Note that 31 August and 16 September followed downwelling winds (positive), and 3 and 10 September were during a period of prolonged upwelling-favorable winds (negative). See Fig. 1 for location of transect and wind measurements.

Table 1. Summary of conditions for 2020 cruises. Wind forcing is based on the mean north–south component of the wind over the preceding 1.5 d ($\sim$ inertial period) prior to the survey. Mean winds from the south are considered upwelling, and mean winds from the north are considered downwelling. Only data from the central transect shown in Fig. 1 are reported. Mean BBL height, mean $\partial T/\partial z$, and max$\partial T/\partial z$ are the average values for all profiles collected on the transect ($n \sim 11$). BBL height is estimated from the vertical location where the maximum value of $\partial T/\partial z$ is observed. The normalized hypoxic volume is calculated as the vertical and across-shelf extent of water with DO concentration $< 3\,\mathrm{mg\,L^{-1}}$ and is normalized by distance in the along-isobath direction (e.g., units of area).

Survey date (2020)	Preceding wind forcing	Mean BBL height [m]	Normalized hypoxic volume [$\mathrm{m^3\,m^{-1}}$]	Mean $\partial T/\partial z$ [$^\circ\mathrm{C\,m^{-1}}$]	Max. $\partial T/\partial z$ [$^\circ\mathrm{C\,m^{-1}}$]	Correlation OBS–fluorometer [r]	Slope OBS–fluorometer [$\mu\mathrm{g\,L^{-1}\,NTU^{-1}}$]
31 Aug	Downwelling	4.23	11 400	0.28	3.45	0.80	25.3
3 Sep	Upwelling	8.09	19 760	0.39	2.90	0.83	21.9
10 Sep	Upwelling	11.47	11 970	0.56	3.00	0.91	27.3
16 Sep	Downwelling	6.09	27 930	0.18	4.92	0.52	12.4
24 Sep	Downwelling	18.43	n/a	0.07	0.98	0.84	6.4

n/a: not applicable.

of moderate northerly winds, and a strong bottom density front had formed during these downwelling-favorable conditions, with a much thinner BBL than was observed 6 d prior (Fig. 3k). Following this northerly wind event, the overall volume of hypoxic water increased by roughly a factor of 2 compared to the previous survey. Chlorophyll fluorescence was concentrated in a much thinner layer following winds from the north (e.g., 31 August and 16 September), and a much sharper thermocline was observed. A strong and prolonged northerly wind event in late September largely mixed the water column, and no hypoxia was observed during a survey on 24 September 2020 (Fig. 3n).

During all cruises, optical backscatter was highest in subpycnocline waters (Fig. 3), and there was a statistically significant ($p < 0.01$) positive correlation between optical backscatter and chlorophyll fluorescence (Table 1). These data suggest that phytoplankton in the water column were the primary component of the suspended particulate material detected by the OBS. However, the nature of the relationship between the OBS data and fluorescence changed between the cruises, and the slope of the linear regression between these two quantities decreased by more than a factor of 2 between the 10 and 16 September surveys. This decrease in slope is consistent with the wanning stages of a bloom, in which the suspended particulate matter is composed primarily of dead or weakly fluorescing cells. The optical backscatter data suggest that these cells are found almost exclusively below the thermocline and may be the primary source of the biological oxygen demand (BOD) that is depleting bottom waters of DO.

The hydrographic surveys highlight that the across-shelf density structure in CCB responds in a manner that is consistent with upwelling/downwelling following winds from the south/north. This could be a local response in which winds from the north/south are balanced by the sea-surface slope, which drives a geostrophic along-isobath interior flow. This along-isobath interior flow would drive bottom Ekman transport that results in upwelling for winds from the south and downwelling for winds from the north. Alternatively, the across-shelf density structure in CCB may be driven remotely by the response along the open coastline to the north. Allen (1976) suggests that upwelling/downwelling propagates as a coastally trapped wave; thus CCB may be driven by the larger-scale response along the open New England coastline. Over this region, the coastline is orientated roughly parallel to southwest–northeast winds, with southwest winds driving upwelling and northeast winds driving downwelling. While the exact dynamics that drive this response are beyond the scope of this paper, our data clearly demonstrate that the density structure responds strongly to the north–south component of the wind.

The impact of upwelling/downwelling on the density structure can be seen more clearly by comparing individual profiles collected on 10 (after upwelling) and 16 September (after downwelling) from the same mid-shelf location (Fig. 4). Although winds from the south and the resulting upwelling increased the overall top-to-bottom temperature difference, the resulting thermocline was much more diffuse, with a maximum local temperature gradient in the thermocline of $\sim 2\,^\circ\mathrm{C\,m^{-1}}$. In contrast, after downwelling conditions, the overall top-to-bottom temperature difference was reduced, but the thermocline was both locally more intense ($> 10\,^\circ\mathrm{C\,m^{-1}}$) and closer to the seabed. These trends are not limited to this one station but are reflected in the across-shelf average of all stations (Table 1). On average, upwelling conditions (3 and 10 September) increase the mean temperature gradient, but downwelling winds (31 August and 16 September) increase the maximum value of the temperature gradient in the thermocline and decrease the BBL height. In these data, a discrete sub-surface chlorophyll maximum was associated with a sharper and more intense thermocline following downwelling, and low-DO bottom waters were associ-

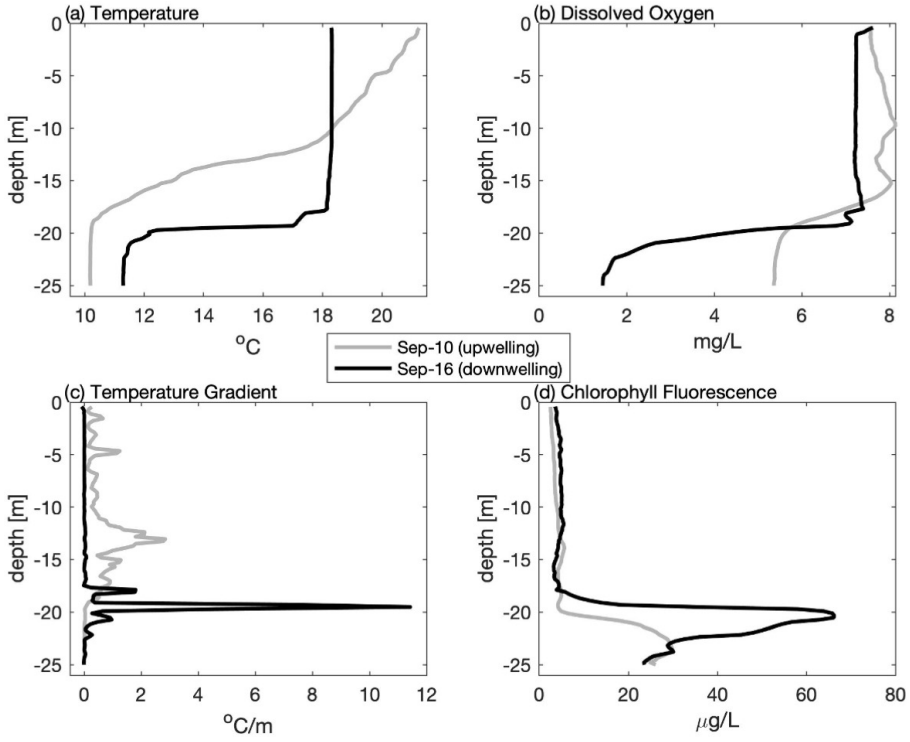

Figure 4. Vertical profiles from the mid-shelf ($\sim 41.82°$ N) collected during late summer 2020 including **(a)** temperature, **(b)** dissolved oxygen, **(c)** vertical temperature gradient, and **(d)** chlorophyll fluorescence highlighting the difference following upwelling (10 September grey line) and downwelling (16 September black line) conditions. Note that even though the top-to-bottom temperature difference is greater following upwelling, downwelling results in a stronger temperature gradient, thinner bottom boundary layer, lower dissolved oxygen, and higher sub-surface chlorophyll fluorescence.

ated with a thin BBL. Thus, moderate downwelling events may result in conditions that are more favorable to both sub-surface phytoplankton production and bottom hypoxia.

A notable feature of the 2020 data is the sub-surface chlorophyll maximum that is seen in the across-shelf surveys. To put these data into context, we compare them to the longer time series of chlorophyll fluorescence collected by CCS in CCB, which covers the period 2011–2020. The data from 2019 and 2020 are remarkable because they have some of the highest fluorescence values observed during the 10-year record, and these values are often found in discrete sub-surface maxima (Fig. 5). For example, in September 2020 a sub-surface maximum with chlorophyll fluorescence $\sim 100\,\mu g\,L^{-1}$ was observed at station 9N (Fig. 5g). Prior to 2019, the highest value recorded anywhere in the water column in September at this station was $\sim 8\,\mu g\,L^{-1}$. While no CCS data were collected in August 2019, the August 2020 bay-wide, eight-station average of depth-integrated chlorophyll fluorescence was the highest ever recorded. Both September 2019 and 2020 had more than 3 times the integrated chlorophyll, on average, than the September mean prior to 2019 (Fig. 6a). This dramatic increase in the late-summer integrated chlorophyll values for 2019–2020 is likely a key contributor to the occurrence of hypoxia during those years. If we convert the average August–September depth-integrated chlorophyll to carbon biomass using a carbon-to-chlorophyll ratio of ~ 60 (see below), the average values for the periods 2011–2018 and 2019–2020 are 225 and 745 mmol C m^{-2}, respectively. If we further assume that all of this biomass is respired in a BBL that is ~ 5 m thick, this represents a BOD of 45 and 149 mmol O_2 m^{-3} (1.4 and 4.8 mg L^{-1}), respectively. Given that bottom summer DO levels typically average 156–188 mmol O_2 m^{-3} (5–6 mg L^{-1}), this dramatic increase in chlorophyll biomass readily explains the switch from normoxic to hypoxic conditions given the major increase in BOD starting in 2019. It is important to note that it does not matter whether the respiration of this excess organic matter occurs in the sub-pycnocline water column or the benthos. Both will deplete bottom waters of DO when a strong thermocline is present. The 2020 survey data show elevated levels of optical backscatter below the thermocline that are likely dominated by post-bloom phytoplankton cells, which are the most likely source of BOD in the BBL.

The anomalously high chlorophyll fluorescence in 2019 and 2020 was accompanied by anomalously low bottom nutrients (Fig. 6b). Bottom nutrient data collected by CCS for the period 2011–2020 were used to estimate the total

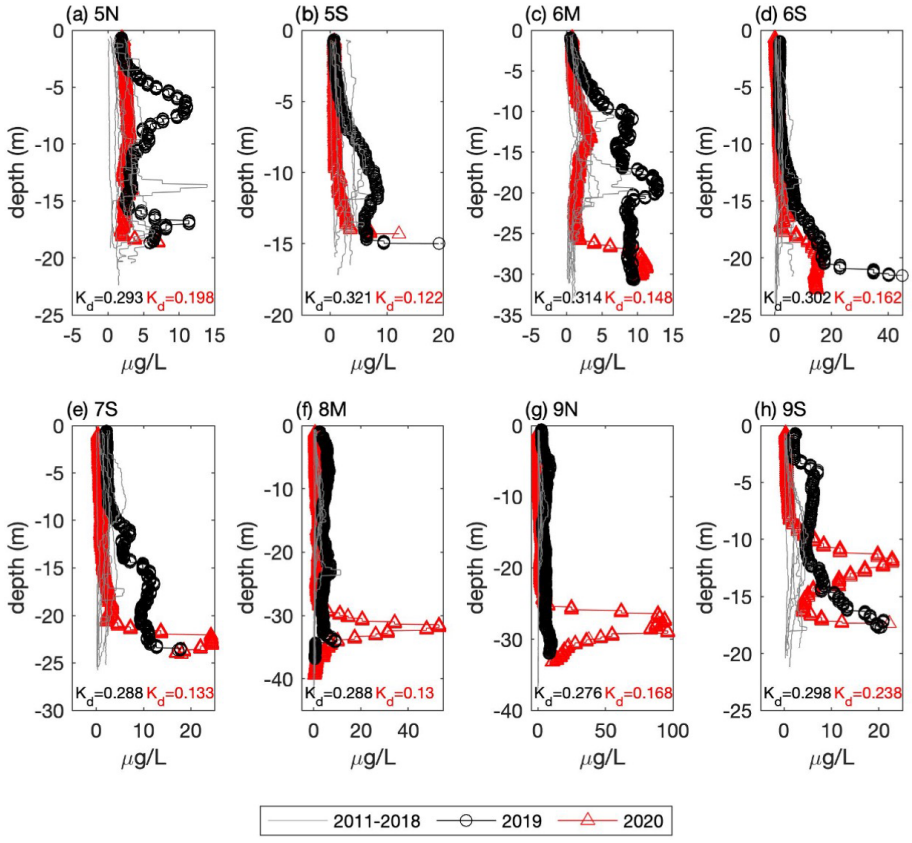

Figure 5. Vertical profiles of chlorophyll fluorescence from the September CCS cruises for all eight CCB stations (see Fig. 1 for locations). Data from 2011–2018 are plotted as grey lines and 2019 and 2020 as circles and triangles, respectively. Estimates of the light attenuation coefficient (K_d) for the 2019 (black) and 2020 (red) profiles are reported at the bottom of each plot.

integrated inorganic nitrogen ($NO_2^- + NO_3^- + NH_4^+$) within the BBL by multiplying the bottom nutrient concentration by the estimated height of the BBL. BBL height was estimated from vertical CTD profiles as the first location above the seabed where the vertical temperature gradient exceeds $1\,°C\,m^{-1}$. Prior to 2019, the bay-wide (eight-station-averaged) BBL-integrated nutrient concentration averaged over August and September was $\sim 67\,mmol\,N\,m^{-2}$. This value drops by more than a factor of 8, on average, for 2019–2020 ($\sim 8\,mmol\,N\,m^{-2}$) consistent with the large increase in integrated fluorescence. There is a significant ($p < 0.05$) negative relationship ($r = -0.89$) between depth-integrated chlorophyll and BBL-integrated nutrients, consistent with increased nutrient consumption resulting in higher chlorophyll biomass. The significance of this relationship is clearly driven by the anomalously high chlorophyll and anomalously low nutrients in late summer 2019 and 2020, and the negative correlation is not significant if these 2 years are excluded ($r = -0.28$, $p = 0.5$). The slope of the linear regression between the integrated nutrients and chlorophyll is $-1.32\,mg\,chl\,(mmol\,N)^{-1}$. If nutrient uptake is consistent with the Redfield ratio, this analysis implies a carbon-to-chlorophyll ratio of $\sim 60\,mg\,C\,(mg\,chl)^{-1}$, which falls well within the range of reported values (e.g., Sathyendranath et al., 2009).

This relatively abrupt shift in sub-pycnocline nutrient utilization is consistent with a significant physical alteration of the late-summer phytoplankton niche in CCB, which we hypothesize to have resulted in the recent emergence of a new phytoplankton species – *K. mikimotoi*. The MWRA has been sampling and quantifying phytoplankton species since 1992 at ~ 40 stations throughout the region. Prior to 2017, *K. mikimotoi* had never been found in any sample collected as part of this monitoring program. In September 2017, *K. mikimotoi* was first detected in samples collected in CCB (F01 and F02, see Fig. 1 for locations). Low levels ($\sim 2500\,cells\,L^{-1}$) of *K. mikimotoi* were again detected in summer 2018, before increasing by over an order of magnitude in late summer 2019 and 2020 (Fig. 6c and Table S1 in the Supplement). Maximum counts of *K. mikimotoi* at station F01 in late-summer surface samples were 74 676 and 138 559 cells L^{-1} in 2019 and 2020, respectively. The MWRA only conducts phytoplankton counts on surface samples collected from CCB. However, one bottom sample was collected from station F01 on 31 August 2020, and the *K. mikimotoi* count exceeded 771 000 cells L^{-1}, accounting for over 70 % of the identifi-

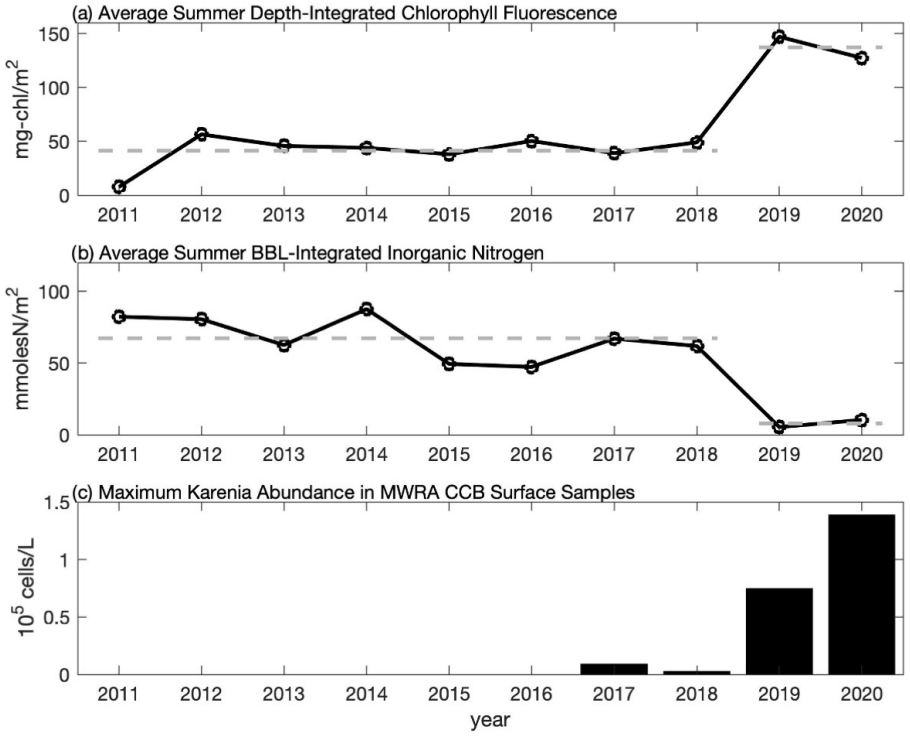

Figure 6. Time series of the average summer **(a)** depth-integrated chlorophyll fluorescence from CCS surveys, **(b)** bottom boundary layer (BBL) integrated inorganic nitrogen from CCS surveys, and **(c)** maximum abundance of *K. mikimotoi* from MWRA late-summer (August and September) surface samples in CCB (F01 and F02). In **(a)** and **(b)** each point represents the average over the August and September CCS cruises and over all eight CCB stations. Average values for 2011–2018 and 2019–2020 are shown with the thick dashed line highlighting that the 2019–2020 data differ by more than a factor of 3 from the 2011–2018 average. In **(c)**, maximum abundance is based on the highest value reported during late summer at either F01 or F02 (see Table S1 for data).

able species at this location. This was the same day that the across-shelf survey documented an intense sub-surface fluorescence maximum (Fig. 3c).

PAR data collected during the CCS cruises suggest that the deep chlorophyll maximum is located near the base of the euphotic zone. Estimates of the light attenuation coefficient (K_d) have a mean value of $0.218\,m^{-1}$ for late summer (August and September), averaged over all stations and all years. This corresponds to a 1 % light level at a depth of ~ -21 m. There is interannual variability and no clear long-term trends in the estimates of K_d. However, September 2019 had the highest values (mean $= 0.298\,m^{-1}$), and September 2020 had the lowest values (mean $= 0.165\,m^{-1}$). This is generally consistent with the intense deep chlorophyll fluorescence observed in 2020 when waters were generally clearer, in contrast to the broadly elevated profiles observed in 2019.

5 Discussion

The data presented above indicate that increased sub-surface chlorophyll production during late summer in 2019 and 2020 has provided the increased biomass to deplete bottom oxygen to hypoxic levels. The CCS nutrient data demonstrate that in the 8 years prior to 2019 there were ample sub-pycnocline nutrients in CCB to support higher productivity, yet late-summer sub-surface blooms of similar magnitude did not develop. We hypothesize that the intense sub-surface blooms that were observed in late summer 2019 and 2020 were *K. mikimotoi* – a dinoflagellate species that had not been detected in the region prior to 2017. The emergence of this new species is consistent with a physical environment that has undergone significant changes. As we will discuss below, these changes include warmer waters, increased thermal stratification, and important shifts in summer wind direction. These changes potentially have resulted in an environment that (1) favors enhanced sub-surface phytoplankton production by motile species and (2) is more physically susceptible to hypoxia.

5.1 Emergence of *K. mikimotoi*

K. mikimotoi had never been detected in MWRA samples prior to 2017 but was detected at numerous locations throughout the GOM in late summer 2017 (Libby et al., 2018). The near-synchronous appearance of this new species most likely reflects a broad introduction by regional circula-

tion. Since 2017, *K. mikimotoi* has been detected consistently in samples collected in CCB. Despite its recent emergence in CCB, we did not collect water samples for species identification from the sub-surface chlorophyll maxima we observed in 2020. The only sub-surface sample collected for phytoplankton identification during late summer 2020 had the highest *K. mikimotoi* counts ever observed in CCB. This sample was collected on the same day (31 August 2020) as the data shown in Fig. 3c, just west of the end of this transect. During this survey, chlorophyll fluorescence was extremely high ($> 150\,\mu g\,L^{-1}$) and almost exclusively contained in a very thin (~ 2 m) layer at the base of the thermocline. This intense sub-surface chlorophyll maximum is consistent with a species that is well-adapted to growth in low light conditions and that can vertically maintain its position in the water column to take advantage of sub-pycnocline nutrients. *K. mikimotoi* is particularly well-adapted to exploit low light environments (Honjo et al., 1991) and can vertically migrate at rates up to $2\,m\,h^{-1}$ (Koizumi et al., 1996). Under stratified conditions migration ceases, and it is often observed in very thin layers within the thermocline (Brand et al., 2012). The recent emergence of late-summer hypoxia also is broadly consistent with the establishment of *K. mikimotoi* as a late-summer bloom species. Hypoxia has been attributed to blooms of *K. mikimotoi* in regions around the world including Japan, China, Norway, Scotland, and Ireland (Tangen, 1977; Matsuyama, 2008; O'Boyle et al., 2016; Li et al., 2019). Oxygen utilization studies indicate that most of the potential BOD from decaying *K. mikimotoi* is realized in the first 5 d of bloom collapse (O'Boyle et al., 2016). This rapid depletion of DO following a bloom results from the highly labile nature of *K. mikimotoi* cells. *K. mikimotoi* has an athecate cell that lacks an armored wall and is easily ruptured, allowing quick release of organic carbon for bacterial respiration (Brand et al., 2012).

5.2 Regional climate change in Cape Cod Bay

The emergence of a new late-summer bloom species is a strong indication that CCB has undergone significant habitat alteration. Consistent with Smayda's (2002) "bloom paradigm," we hypothesize that changes to the physical environment in CCB have allowed *K. mikimotoi* to bloom in late summer. Waters in the GOM are warming more rapidly than nearly any other region in the world's oceans (Pershing et al., 2015). Surface temperature data from the NDBC Boston buoy (44013) show that surface waters are warming even more rapidly in CCB, and 2019 and 2020 were among the warmest summers recorded over the past 36 years (Fig. 7a). Both light-saturated and light-limited growth rates in phytoplankton are sensitive to temperature (Edwards et al., 2016), and the warming of CCB may have increased overall levels of primary production. However, it seems unlikely that the dramatic increase in chlorophyll fluorescence in later summer 2019 and 2020 can be explained simply by increased primary production without significant changes to the late-summer phytoplankton species composition. Species transitions are expected to occur in association with increases in temperature (Eppley, 1972; Norberg, 2004), and the emergence of *K. mikimotoi* may be the result of increased summer water temperature. *K. mikimotoi* can grow over a wide range of temperatures, but the optimal range for blooms is thought to be 20–24 °C (Baohong et al., 2021). Prior to 2015, water in excess of 20 °C at the Boston buoy (44013) averaged roughly 6 d a summer and only exceeded 20 d once (2011). However, during four of the last five summers (2016, 2018, 2019, and 2020), surface temperatures have exceeded this threshold for more than 40 d (Fig. 7b).

Bottom waters at the MDMF Wreck of the Mars location (depth ~ 33 m) also demonstrate significant increases in temperature. However, during the summer months surface water temperatures at the Boston buoy increase at nearly twice the rate as bottom waters in northern Cape Cod Bay (at the Wreck of the Mars site) over the period 1991–2020. While the data collected at the Boston buoy and the Wreck of the Mars are not co-located, the long-term trends at these two sites are consistent with increasing levels of thermal stratification (Fig. 7c). Increased vertical density stratification reduces vertical mixing and the associated nutrient fluxes, favoring motile species such as dinoflagellates that can maintain their vertical position (Winder and Sommer, 2012). Thermal stratification also is significantly impacted by wind forcing. As demonstrated in Fig. 4 and Table 1, moderate downwelling-favorable winds result in a deep and sharp thermocline and a thin BBL. In contrast, winds from the south (upwelling) generally result in a more diffuse thermocline with a thicker BBL. At the Boston buoy (44013) the likelihood of summer winds from the northeast stronger than $7.7\,m\,s^{-1}$ (15 kn) has increased by nearly 10 % per decade (Fig. 7d). This increase in stronger winds from the northeast is largely at the expense of stronger winds from the southwest, which have become much less common during the summer months. This significant increase in downwelling winds during late summer is likely to enhance deeper and stronger near-bed thermal stratification – an environment that may favor a light-adapted motile dinoflagellate species such as *K. mikimotoi*. In 2020, the highest chlorophyll fluorescence was observed when there was a sharp well-defined thermocline – conditions that were observed following downwelling-favorable winds (31 August and 16 September). Upwelling conditions resulted in not only a more diffuse thermocline but a more diffuse vertical distribution of fluorescence as well.

Blooms of the genus *Karenia* are commonly found in coastal regions with strong horizontal density fronts, and it has been suggested that physical convergence is important to bloom formation (Brand et al., 2012). The allelopathy of *K. mikimotoi* increases significantly at high cell concentration (Li et al., 2019), so convergent physical processes may give this relatively slow-growing species a competitive ad-

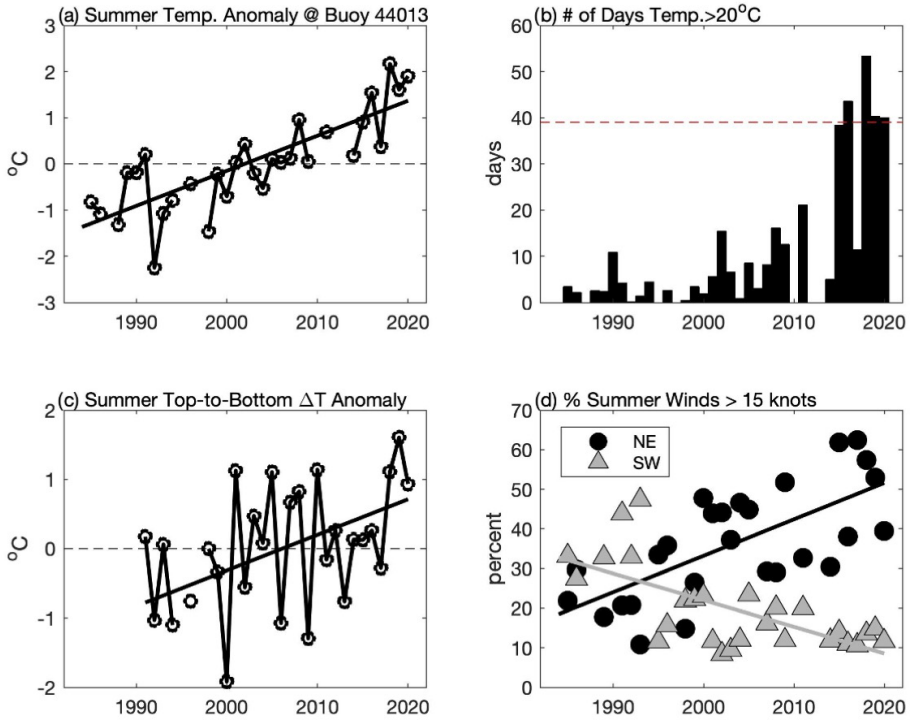

Figure 7. Changes in summer (June–September) conditions in CCB including **(a)** mean surface water temperature anomaly at the NDBC buoy 44013, **(b)** total number of days when surface water temperature exceeded 20 °C at the NDBC buoy 44013, **(c)** temperature difference anomaly between NDBC buoy 44013 (surface) and MDMF Wreck of the Mars (∼ 33 m depth), and **(d)** percentage of time that summer winds in excess of 15 kn (7.7 m s^{-1}) are from the northeast (black circles) and from southwest (grey triangle). Solid lines in **(a)**, **(c)**, and **(d)** are linear regressions, all of which are significant at $p < 0.05$. In **(a)** and **(b)**, the anomalies are simply calculated by removing the mean over the period of record.

vantage. Downwelling-favorable winds drive convergence in bottom Ekman transport, which act to generate a bottom density front (Allen and Newberger, 1996). We observe a strong bottom temperature front following downwelling conditions in CCB (e.g., Fig. 3b and k), consistent with strong physical convergence in this region. The significant increase in moderate downwelling conditions during late summer may have provided a mechanism that has helped physically concentrate *K. mikimotoi*, allowing it to bloom. In contrast, upwelling-favorable conditions generate a surface front and bring nutrients from depth to the surface conditions that are likely to favor faster-growing, immotile species. Thus, the long-term shifts in summer wind patterns, combined with increases in water temperature, may have resulted in an environment that is much more conducive to blooms of this new species. It is worth noting that for large parts of the GOM southwest winds are upwelling-favorable, and the long-term reduction in summer upwelling conditions most likely has contributed to the unprecedented warming of surface waters in the region.

5.3 Physical susceptibility to hypoxia

The overall increase in thermal stratification combined with the significant increase in downwelling-favorable summer winds may have resulted in an environment that also is more physically susceptible to hypoxia. The data collected in 2020 demonstrate that hypoxia develops where strong thermal stratification intersects the seafloor, suppressing vertical mixing and confining the BOD to a very thin BBL (Fennel et al., 2016). The thinnest BBLs and strongest local thermoclines in 2020 were observed following moderate downwelling conditions (e.g., Fig. 4), which helps explain why the overall volume of hypoxic water was reduced following upwelling conditions and increased following downwelling (e.g., Fig. 3). Irrespective of whether the remineralization of organic matter occurs primarily in the water column or via benthic respiration, a thin BBL effectively concentrates BOD over a smaller volume of water, resulting in a more rapid drawdown of bottom DO. Upwelling brings bottom waters into shallower water where greater vertical mixing can take place, potentially ventilating hypoxic bottom waters. We hypothesize that more frequent downwelling events interrupt this process and promote an environment that is more susceptible to hypoxia due to intense near-bed stratification. Even though strong downwelling winds eventually mixed the water column ending hypoxia in both 2019 and 2020, long-term increases in moderate downwelling-favorable winds during the summer, combined with increased overall levels of ther-

mal stratification, may enhance hypoxia by favoring a deep thermocline and thin BBL. The fact that such a thin BBL can be maintained in southern CCB is likely related to the fact that it is a semi-enclosed embayment, which limits the near-bed currents and hence the bottom stress. Along open coastlines, the along-shelf bottom stress evolves to balance the along-shelf wind stress to first order (Lentz and Fewings, 2012). However, in CCB the presence of the shoreline prevents this acceleration, and the wind stress can be balanced by the sea-level setup to first order, significantly reducing the bottom stress. This weak bottom stress, and the corresponding reduction in vertical mixing, is likely a key reason why hypoxia can develop in this environment.

6 Conclusion

For two consecutive summers, bottom waters in CCB have become hypoxic. This unprecedented occurrence appears to be the result of a change in physical conditions that favors the growth of *K. mikimotoi*, a bloom-forming dinoflagellate linked to hypoxia in a number of other coastal environments. Increased water temperatures and thermal stratification, combined with more frequent downwelling-favorable winds, have created an environment where strong vertical stratification is maintained very close the seabed. This results in conditions that are more physically susceptible to hypoxia and may allow certain phytoplankton to more effectively utilize the reservoir of deep sub-pycnocline nutrients. These dramatic changes in CCB illustrate how the complex response to climate change can significantly alter bottom oxygen dynamics and play an important role in controlling the floral composition of a coastal marine ecosystem.

Data availability. The data collected for this project have been archived and are available at https://doi.org/10.26025/1912/29009 (Scully et al., 2022). The National Data Buoy Center (NDBC) buoy 44013 data are available at https://www.ndbc.noaa.gov/station_history.php?station=44013 (US DOC/NOAA/NWS/NDBC, 1971).

Supplement. The supplement related to this article is available online at: https://doi.org/10.5194/bg-19-3523-2022-supplement.

Author contributions. MES was the primary author of the manuscript and participated in all aspects of data collection and analysis reported in this paper. WRG edited the manuscript and assisted with data analysis and interpretation. DB provided the phytoplankton identification data and helped edit the manuscript. TLP edited the manuscript and provided the 2019 bottom dissolved oxygen data and historical bottom temperature data. AC edited the manuscript and provided the historical water quality data for Cape Cod Bay. OCN edited the manuscript and provided assistance with data analysis.

Competing interests. The contact author has declared that none of the authors has any competing interests.

Disclaimer. Publisher's note: Copernicus Publications remains neutral with regard to jurisdictional claims in published maps and institutional affiliations.

Acknowledgements. We are grateful to Marc Costa, captain of the R/V *Columbia*, and Noa Randall for their assistance during the hydrographic surveys. MDMF staff members Alex Boeri, Crystal Cano, Derek Perry, Brenden Reilly, and Steve Wilcox conducted water quality sampling in 2019. We would like to thank the Massachusetts Lobstermen's Association and commercial lobster fishers in southern Cape Cod Bay for alerting us to the 2019 hypoxic event and communicating the conditions they were observing in both 2019 and 2020.

Financial support. This research has been supported by the National Science Foundation (grant no. OCE-2053240) and the National Oceanic and Atmospheric Administration (grant no. NA20OAR4170506).

Review statement. This paper was edited by Tina Treude and reviewed by two anonymous referees.

References

Anderson, D. M., Cembella, A. D., and Hallegraeff, G. M.: Progress in understanding harmful algal blooms: paradigm shifts and new technologies for research, monitoring, and management, Annu. Rev. Mar. Sci., 4, 143–176, 2012.

Allen, J. S.: Some aspects of the forced wave response of stratified coastal regions, J. Phys. Oceanogr., 6, 113–119, 1976.

Allen, J. S. and Newberger, P. A.: Downwelling circulation on the Oregon continental shelf. Part I: Response to idealized forcing, J. Phys. Oceanogr., 26, 2011–2035, 1996.

Baohong, C., Kang, W., Huige, G., and Hui, L.: Karenia mikimotoi blooms in coastal waters of China from 1998 to 2017, Estuar. Coast. Shelf S., 249, 107034, 2021.

Bjørnsen, P. K. and Nielsen, T. G.: Decimeter scale heterogeneity in the plankton during a pycnocline bloom of Gyrodinium aureolum, Mar. Ecol.-Prog. Ser., 263–267, 1991.

Brand, L. E., Campbell, L., and Bresnan, E.: Karenia: The biology and ecology of a toxic genus, Harmful Algae, 14, 156–178, 2012.

Borkman, D.: Phytoplankton and Nutrients in Buzzards Bay, Massachusetts 1987–1988, MS Thesis, University of Massachusetts Dartmouth, Dartmouth, MA, 203 pp, 1994.

Borkman, D., Pierce, R. W., and Turner, J. T.: Dinoflagellate blooms in Buzzards Bay, Massachusetts, in: Proceedings of the Fifth International Conference on Toxic Marine Phytoplankton, edited by: Smayda, T. J. and Shimizu, Y., Elsevier, 211–216, 1993.

Costa, A., Larson, E., and Stamieszkin, K.: Quality Assurance Project Plan (QAPP) for water quality monitoring in Cape

Cod Bay, 2020–2022, Massachusetts Water Resources Authority, Boston, Report 2020-07, p 88, 2020.

Dahl, E. and Brockmann, U. H.: Does Gyrodinium aureolum Hulbert perform diurnal vertical migrations?, in: Red Tides: Biology, Environmental Science, and Toxicology, edited by: Okaichi, T., Anderson, D. M., and Nemoto, T., Elsevier, New York, 225–22, 1989.

Diaz, R. J.: Overview of hypoxia around the world, J. Environ. Qual., 30, 275–281, 2001.

Edwards, K. F., Thomas, M. K. Klausmeier, C. A., and Litchman, E.: Phytoplankton growth and the interaction of light and temperature: A synthesis at the species and community level, Limnol. Oceanogr., 61, 1232–1244, 2016.

Eppley, R. W.: Temperature and phytoplankton growth in the sea, Fish. B.-NOAA, 70, 1063–1085, 1972.

Falkowski, P. G. and Oliver, M. J.: Mix and match: how climate selects phytoplankton, Nat. Rev. Microbiol., 5, 813–819, 2007.

Fennel, K. and Testa, J. M.: Biogeochemical controls on coastal hypoxia, Annu. Rev. Mar. Sci., 11, 105–130, 2019.

Fennel, K., Laurent, A., Hetland, R., Justić, D., Ko, D. S., Lehrter, J., Murrell, M., Wang, L., Yu, L., and Zhang, W.: Effects of model physics on hypoxia simulations for the northern Gulf of Mexico: A model intercomparison, J. Geophys. Res.-Oceans, 121, 5731–5750, 2016.

Forrest, D. R., Hetland, R. D., and DiMarco, S. F.: Multivariable statistical regression models of the areal extent of hypoxia over the Texas–Louisiana continental shelf, Environ. Res. Lett., 6, 045002, https://doi.org/10.1088/1748-9326/7/1/019501, 2011.

García-Reyes, M., Sydeman, W. J., Schoeman, D. S., Rykaczewski, R. R., Black, B. A., Smit, A. J., and Bograd, S. J.: Under pressure: Climate change, upwelling, and eastern boundary upwelling ecosystems, Frontiers in Marine Science, 2, 109, https://doi.org/10.3389/fmars.2015.00109, 2015.

Geyer, W. R., Gardner, G. B., Brown, W. S., Irish, D., Butman, B., Loder, T. C., and Signell, R. P.: Physical Oceanographic investigation of Massachusetts and Cape Cod Bays, The Massachusetts Environmental Trust, http://pubs.er.usgs.gov/publication/70196621 (last access: 15 July 2022), 1992.

Grantham, B. A., Chan, F., Nielsen, K. J., Fox, D. S., Barth, J. A., Huyer, A., Lubchenco, J., and Menge, B. A.: Upwelling-driven nearshore hypoxia signals ecosystem and oceanographic changes in the northeast Pacific, Nature, 429, 749–754, 2004.

Griffith, A. W. and Gobler,C. J.: Harmful algal blooms: a climate change co-stressor in marine and freshwater ecosystems, Harmful Algae, 91, 101590, https://doi.org/10.1016/j.hal.2019.03.008, 2020.

Honjo, T., Yamaguchi, M., Nakamure, O., Yamamoto, S., Ouchi, A., and Ohwada, K.: A Relationship between Winter Water Temperature and the Timing of Summer Gymnodinium nagasakiense Red Tides in Gokasho Bay, Nippon Suisan Gakkai Shi, 57, 679–1682, 1991.

Huisman, J., Sharples, J., Stroom, J. M., Visser, P. M., Kardinaal, W. E. A., Verspagen, J. M., and Sommeijer, B.: Changes in turbulent mixing shift competition for light between phytoplankton species, Ecology, 85, 2960–2970, 2004.

Hunt, C. D., Borkman, D. G., Libby, P. S., Lacouture, R., Turner, J. T., and Mickelson, M. J.: Phytoplankton patterns in Massachusetts Bay – 1992–2007, Estuar. Coast., 33, 448–470, 2010.

Jiang, M., Zhou, M., Libby, S., and Hunt, C. D.: Influences of the Gulf of Maine intrusion on the Massachusetts Bay spring bloom: A comparison between 1998 and 2000, Cont. Shelf Res., 27, 2465–2485, 2007.

Koizumi, Y., Uchida, T., and Honjo, T.: Diurnal vertical migration of Gymnodinium mikimotoi during a red tide in Hoketsu Bay, Japan, J. Plankton Res., 18, 289–294, 1996.

Kudela, R. M., Seeyave, S., and Cochlan, W. P.: The role of nutrients in regulation and promotion of harmful algal blooms in upwelling systems, Prog. Oceanogr., 85, 122–135, 2010.

Lentz, S. J. and Fewings, M. R.: The wind-and wave-driven inner-shelf circulation, Annu. Rev. Mar. Sci., 4, 317–343, 2012.

Li, X., Yan, T., Yu, R., and Zhou, M.: A review of Karenia mikimotoi: Bloom events, physiology, toxicity and toxic mechanism, Harmful Algae, 90, 101702, https://doi.org/10.1016/j.hal.2019.101702, 2019.

Libby, P. S., Borkman, D. G., Geyer, W. R., Turner, J. T., Costa, A. S., Wang, J., and Codiga, D.: 2017 Water column monitoring results, Massachusetts Water Resources Authority, Boston, Report 2018-04, p. 59, https://www.mwra.com/harbor/enquad/pdf/2018-04.pdf (last access: 7 July 2022), 2018.

Libby, P. S., Borkman, D. G., Geyer, W. R., Turner, J. T., Costa, A. S., Taylor, D. I., Wang, J., and Codiga, D.: 2019 Water column monitoring results, Boston: Massachusetts Water Resources Authority, Report 2020-08, p. 60, https://www.mwra.com/harbor/enquad/pdf/2020-08.pdf (last access: 15 July 2022), 2020.

Matsuyama, Y.: Red tide due to the dinoflagellate *Karenia mikimotoi* in Hiroshima Bay 2002: environmental features during the red tide and associated fisheries damages to finfish and shellfish aquaculture, in: Proceedings of the 12th International Conference on Harmful Algae, International Society for the Study of harmful Algae and International Oceanographic Commission of UNESCO Copenhagen, 209–211, 2008.

Norberg, J.: Biodiversity and ecosystem functioning: a complex adaptive systems approach, Limnol. Oceanogr., 49, 1269–1277, 2004.

O'Boyle, S., McDermott, G., Silke, J., and Cusack, C.: Potential impact of an exceptional bloom of Karenia mikimotoi on dissolved oxygen levels in waters off western Ireland, Harmful Algae, 53, 77–85, 2016.

Oviatt, C. A., Hyde, K. J., Keller, A. A., and Turner, J. T.: Production patterns in Massachusetts Bay with outfall relocation, Estuar. Coast., 30, 35–46, 2007.

Pershing, A. J., Alexander, M. A., Hernandez, C. M., Kerr, L. A., Le Bris, A., Mills, K. E., Nye, J. A., Record, R., Scannell, H. A., Scott, J. D., and Sherwood, G. D.: Slow adaptation in the face of rapid warming leads to collapse of the Gulf of Maine cod fishery, Science, 350, 809–812, 2015.

Riegman, R., Boer, M. D., and Domis, L. D. S: Growth of harmful marine algae in multispecies cultures, J. Plankton Res., 18, 1851–1866, 1996.

Sathyendranath, S., Stuart, V., Nair, A., Oka, K., Nakane, T., Bouman, H., Forget, M. H., Maass, H., and Platt, T.: Carbon-to-chlorophyll ratio and growth rate of phytoplankton in the sea, Mar. Ecol.-Prog. Ser., 383, 73–84, 2009.

Schultz, M. and Kiørboe, T.: Active prey selection in two pelagic copepods feeding on potentially toxic and non-toxic dinoflagellates, J. Plankton Res., 31, 553–561, 2009.

Scully, M. E.: The importance of climate variability to wind-driven modulation of hypoxia in Chesapeake Bay, J. Phys. Oceanogr., 40, 1435–1440, 2010.

Scully, M. E.: The contribution of physical processes to inter-annual variations of hypoxia in Chesapeake Bay: A 30-yr modeling study, Limnol. Oceanogr., 61, 2243–2260, 2016.

Scully, M. E., Pugh, T. L., Geyer, W. R., Costa, A., Nichols, O. C.: Southern Cape Cod Bay hypoxia data, WHOAS [data set], https://doi.org/10.26025/1912/29009, 2022.

Signell, R. P., Jenter, H. L., and Blumberg, A. F.: Predicting the physical effects of relocating Boston's sewage outfall, Estuar. Coast. Shelf S., 50, 59–71, 2000.

Smayda, T. J.: Adaptive ecology, growth strategies and the global bloom expansion of dinoflagellates, J. Oceanogr., 58, 281–294, 2002.

Smayda, T. J. and Reynolds, C. S.: Community assembly in marine phytoplankton: application of recent models to harmful dinoflagellate blooms, J. Plankton Res., 23, 447–461, 2001.

Tangen, K.: Blooms of Gyrodinium aureolum (Dinophyceae) in North European waters, accompanied by mortality in marine organisms, Sarsia, 63, 123–133, 1977.

Tilzer, M. M., Gieskes, W. W., and Beese, B.: Light-temperature interactions in the control of photosynthesis in Antarctic phytoplankton, Polar Biol., 5, 105–111, 1986.

Turner, J. T., Borkman, D. G., and Pierce, R. W.: Should Red Tide Dinoflagellates be Sampled Using Techniques for Microzooplankton Rather than Phytoplankton?, in: Harmful Marine Algal Blooms, edited by: Lassus, P., Lavoisier, Paris, France, 737–742, 1995.

Uchida, T., Toda, S., Matsuyama, Y., Yamaguchi, M., Kotani, Y., and Honjo, T.: Interactions between the red tide dinoflagellates *Heterocapsa circularisquama* and *Gymnodinium mikimotoi* in laboratory culture, J. Exp. Mar. Biol. Ecol., 241, 285–299, 1999.

US DOC/NOAA/NWS/NDBC (National Data Buoy Center): Meteorological and oceanographic data collected from the National Data Buoy Center Coastal-Marine Automated Network (C-MAN) and moored (weather) buoys [Buoy 44103], NOAA National Centers for Environmental Information [data set], https://www.ndbc.noaa.gov/station_history.php?station=44013 (last access: 1 February 2022), 1971.

Wells, M. L., Karlson, B., Wulff, A., Kudela, R., Trick, C., Asnaghi, C., Berdalet, E., Cochlan, W.,Davidson, K., De Rijcke, M., and Dutkiewicz, S.: Future HAB science: Directions and challenges in a changing climate, Harmful Algae, 91, 101632, https://doi.org/10.1016/j.hal.2019.101632, 2020.

Wilson, R. E., Swanson, R. L., and Crowley, H. A.: Perspectives on long-term variations in hypoxic conditions in western Long Island Sound, J. Geophys. Res.-Oceans, 113, C12011, https://doi.org/10.1029/2007JC004693, 2008.

Winder, M. and Sommer, U.: Phytoplankton response to a changing climate, Hydrobiologia, 698, 5–16, 2012.

Xue, P., Chen, C., and Beardsley, R. C.:. Observing system simulation experiments of dissolved oxygen monitoring in Massachusetts Bay, J. Geophys. Res.-Oceans, 117, C05014, https://doi.org/10.1029/2011JC007843, 2012.

Yu, L., Fennel, K., and Laurent, A.: A modeling study of physical controls on hypoxia generation in the northern Gulf of Mexico, J. Geophys. Res.-Oceans, 120, 5019–5039, 2015.